Scalar isoscalar mesons and the scalar glueball from radiative J/ψ decays

A.V. Sarantsev^{a,b}, I. Denisenko^c, U. Thoma^a, and E. Klempt^a

^aHelmholtz-Institut für Strahlen- und Kernphysik, Universität Bonn, Germany ^bNRC "Kurchatov Institute", PNPI, Gatchina 188300, Russia ^c Joint Institute for Nuclear Research, Joliot-Curie 6, 141980 Dubna, Moscow region, Russia

Abstract

A coupled-channel analysis of BESIII data on radiative J/ψ decays into $\pi\pi$, $K\bar{K}$, $\eta\eta$ and $\omega\phi$ has been performed. The partial-wave amplitude is constrained by a large number of further data. The analysis finds ten isoscalar scalar mesons. Their masses, widths and decay modes are determined. The scalar mesons are interpreted as mainly SU(3)-singlet and mainly octet states. Octet isoscalar scalar states are observed with significant yields only in the 1500-2100 MeV mass region. Singlet scalar mesons are produced over a wide mass range but their yield peaks in the same mass region. The peak is interpreted as scalar glueball. Its mass and width are determined to $M=1865\pm25^{+10}_{-30}$ MeV and $\Gamma=370\pm50^{+30}_{-20}$

A coupled-channel analysis of BESIII data on radiative J/γ partial-wave amplitude is constrained by a large number of Their masses, widths and decay modes are determined. The mainly octet states. Octet isoscalar scalar states are observegion. Singlet scalar mesons are produced over a wide mapeak is interpreted as scalar glueball. Its mass and width an MeV, its yield in radiative J/ψ decays to (5.8 ± 1.0) 10⁻³.

1. Introduction

Scalar mesons – mesons with the quantum numbers of the vacuum – are most fascinating objects in the field of strong interactions. The lowest-mass scalar meson f₀(500), traditionally often called σ, reflects the symmetry breaking of strong interactions and plays the role of the Higgs particle in quantum chromodynamics (QCD) [1, 2]. The f₀(500) is accompanied by further low-mass scalar mesons filling a nonet of particles with spin J = 0 and parity P = +1: The three charge states a₀(980), f₀(500) are supposed to be dynamically generated from meson-meson interactions [3]. Alternatively - or complementary - these mesons are interpreted as four-quark or tetraquark states [4].

The continued quest for scalar isoscalar mesons at higher masses is driven by a prediction – phrased for the first time nearly 50 years ago [5, 6] – that QCD allows for the existence of quark-less particles called glueballs. Their existence is a direct consequence of the nonabelian nature of QCD and of confinement. However, the strength of the strong interaction in the confinement region forbids analytical solutions of full QCD. First quantitative estimates of glueball masses were given in a bag model [7]. Closer to OCD are calculations on a lattice. In quenched ap-

of glueball masses were given in a bag model [7]. Closer to QCD are calculations on a lattice. In quenched approximation, i.e. when $q\bar{q}$ loops are neglected, the lowestmass glueball is predicted to have scalar quantum numbers, and to have a mass in the 1500 to 1800 MeV range [8– 10; unquenching lattice QCD predicts a scalar glueball at $(1795 \pm 60) \,\mathrm{MeV}$ [11]. Exploiting a QCD Hamiltonian in Coulomb gauge generating an instantaneous interaction, Szczepaniak and Swanson [12] calculate the low-lying glueball masses with no free parameters. The scalar glueball of lowest mass is found at 1980 MeV. Huber, Fischer and Sanchis-Alepuz [13] calculate the glueball spectrum using a parameter-free fully self-contained truncation of Dyson-Schwinger and Bethe-Salpeter equations and determine the lowest-mass scalar glueball to $(1850 \pm 130) \,\mathrm{MeV}$. In gravitational (string) theories – an analytic approach to QCD – glueballs are predicted as well [14] at 1920 MeV. Glueballs are predicted consistently within a variety of approaches to QCD. They seem to be a safe prediction.

Scalar glueballs are embedded into the spectrum of scalar isoscalar mesons. These have isospin I=0, positive G-parity (decaying into an even number of pions), their total spin J vanishes, their parity P and their C-parity are positive: $(I^G)J^{PC} = (0^+)0^{++}$. Scalar glueballs have the same quantum numbers as scalar isoscalar mesons and may mix with them. In quark models, mesons are described as bound states of a quark and an antiquark. Their quantum numbers are often defined in spectroscopic notation by the orbital angular momentum of the quark and the antiquark L, the total quark spin S, and the total angular momentum J. Scalar mesons have ${}^{2s+1}L_J = {}^{3}P_0$.

Experimentally, the scalar glueball was searched for intensively but no generally accepted view has emerged. The most promising reaction to search for glueballs are radiative decays of J/ψ . In this process, the dominant contribution to direct photon production is expected to come from the process $J/\psi \rightarrow \gamma$ plus two gluons, where the final-state hadrons are produced by the hadronization of the two gluons. QCD predicts the two gluons to interact forming glueballs - if they exist. Lattice gauge calculations predict a branching ratio for radiative J/ψ decays to produce the scalar glueball of $(3.8\pm0.9)10^{-3}$ [15]. This is a significant fraction of all radiative J/ψ decays ($\approx 13.5\%$). There was hence great excitement when a broad bump in the radiatively produced $\eta\eta$ mass spectrum [16] was discovered by the Crystal Ball collaboration at the Stanford Linear Accelerator (even though with tensor quantum numbers). However, a resonance with the reported properties was not reproduced by any other experiment. The DM2 collaboration reported a strong peak at 1710 MeV in the $K\bar{K}$ invariant mass distribution [17], a peak that is now known as $f_0(1710)$. Data from the CLEO experiment on radiative J/ψ decays into pairs of pseudoscalar mesons were studied in a search for glueballs [18] but no definite conclusions were obtained.

The data with the highest statistics nowadays stem from BESIII in Bejing. The partial wave amplitudes for J/ψ radiative decays into $\pi\pi$ [19] and K_SK_S [20] were determined in fits to the data in slices in the invariant mass of the two outgoing mesons. Data on $J/\psi \to \gamma\eta\eta$ [21] and $J/\psi \to \gamma\phi\omega$ [22] were presented including an interpretation within a partial wave analysis. In the reactions $J/\psi \to \gamma 2\pi^+ 2\pi^-$ [23, 24] and $J/\psi \to \gamma\omega\omega$ [25], the $2\pi^+ 2\pi^-$ and into $\omega\omega$ branching ratios of contributing resonances were deduced from a smaller data sample.

A new understanding of the spectrum of light-quark scalar mesons emerged from the results obtained with the Crystal Barrel experiment at the Low-Energy Antiproton Ring at CERN. In $\bar{p}p$ annihilation at rest, annihilation into $3\pi^0$ [26], $\pi^0\eta\eta$ [27], $\pi^0\eta\eta'$ [28], and $\pi^0K_LK_L$ [29] was studied. These data established the existence of the $f_0(1500)$ resonance; the existence of the $f_0(1370)$ had been proposed in 1966 [30] but its existence was accepted only after its rediscovery at LEAR in $\bar{p}p$ [31] and $\bar{p}n$ annihilation [32, 33].

Central production in hadron-hadron collisions is mostly interpreted as collision of two Pomerons, and this process is supposed to be gluon-rich. Data on this reaction were taken at CERN by the WA102 collaboration that reported results on $\pi^+\pi^-$ and K_SK_S [34], $\eta\eta$ [35], $\eta\eta'$ and $\eta'\eta'$ [36], and into four pions [37]. The GAMS collaboration reported a study of the $\pi^0\pi^0$ system in the charge-exchange reactions $\pi^- p \to \pi^0 \pi^0 n, \eta \eta n$ and $\eta \eta' n$ at $100 \,\mathrm{GeV/c}$ [38] in a mass range up to $3 \,\mathrm{GeV}$. The charge exchange reaction $\pi^- p \to K_S K_S n$ was studied at the Brookhaven National Laboratory [39]. An energy-dependent partial-wave analysis based on a slightly increased data set was reported in Ref. [40]. A reference for any analysis in light-meson spectroscopy are the amplitudes for $\pi\pi \to \pi\pi$ elastic scattering [41]. The low-mass $\pi\pi$ interactions are known precisely from the K_{e4} of charged kaons [42]. In these experiments, a series of scalar isoscalar mesons was found. The Review of Particle Properties (RPP) [43] lists nine states; only the five states at lower mass are considered to be established. None of these states sticks out and identifies itself as the scalar glueball of lowest mass.

Amsler and Close [44, 45] suggested that the three scalar resonances $f_0(1370)$, $f_0(1500)$ and $f_0(1710)$ could originate from a mixing of the scalar glueball with a scalar $\frac{1}{\sqrt{2}}(u\bar{u}+d\bar{d})$ and a scalar $s\bar{s}$ state. A large number of follow-up papers suggested different mixing schemes based on these three mesons. We mention here one recent paper [46] that takes into account the production charac-

teristics of these three mesons in radiative J/ψ decays. However, doubts arose whether a comparatively narrow $f_0(1370)$ exists [47, 48]. Klempt and Zaitsev [47] suggested that the resonances $f_0(1500)$, $f_0(1710)$, $f_0(2100)$ could be SU(3) octet states while the singlet states merge to a continuous scalar background. This continuous scalar background was interpreted as scalar glueball by Minkowski and Ochs (and called red dragon) [49]. In Refs. [50, 51], a fourth isoscalar scalar meson was identified at 1530^{+90}_{-250} MeV with $560 \pm 140 \,\mathrm{MeV}$ width. This broad state was interpreted as glueball. Bugg, Peardon and Zou [52] suggested that the four known mesons $f_0(1500)$, $f_2(1980)$, $f_0(2105)$, $\eta(2190)$ should be interpreted as scalar, tensor, excited scalar and pseudoscalar glueball. Recent reviews of scalar mesons and the scalar glueball can be found elsewhere [47, 53–56].

2. Our data base

It seems obvious that the scalar glueball can be identified reliably only once the spectrum of scalar mesons is understood into which the glueball is embedded. Decisive for the interpretation are the data on radiative J/ψ decays. But many experiments contribute to our knowledge on scalar isoscalar mesons and provide additional constraints. In this coupled-channel analysis we fit mesonpairs in S-wave from radiative J/ψ decays and include the S-wave contributions to $\pi\pi$ elastic scattering [38] and $\pi\pi \to K_SK_S$ [39, 40], the CERN-Munich [41] data and the $K_{\rm e4}$ [42] data. Further, we use 15 Dalitz plots for different reactions from $\bar{p}N$ annihilation at rest [26, 27, 29], [57]-[63].

The real and imaginary parts of the mass-dependent S-wave amplitudes were derived for $J/\psi \to \gamma \pi^0 \pi^0$ in Ref. [19] and $J/\psi \to \gamma K_S K_S$ in Ref. [20]. Assuming dominance of resonances with spin J=0 and J=2, the partial-wave analysis returned - for each mass bin - two possible solutions, called black (b) and red (r). In some mass regions, the two amplitudes practically coincide. We assume continuity between regions in which the two amplitudes are similar, and divide the full mass range into five regions: in three regions, the two amplitudes are identical, in two regions, the red and black amplitudes are different. Thus there are four sets of amplitudes, (r,r); (r,b); (b,r); (b,b). For the data on $J/\psi \to \gamma K_S K_S$, we again define five mass regions and four sets of amplitudes. The red amplitudes (r,r) give the best χ^2 for $\pi\pi$, and (b,b) for $K_S K_S$.

Figure 1a,b shows the $\pi^0\pi^0$ [19] and K_SK_S [20] invariant mass distributions from radiative J/ψ decays for the best set of amplitudes. The "data" are represented by triangles with error bars, the solid curve represents our fit. (i) The $\pi^0\pi^0$ invariant mass distribution shows rich structures. So far, no attempt has been reported to understand the data within an energy-dependent partial-wave analysis. The mass distribution starts with a wide enhancement at about 500 MeV and a narrow peak at

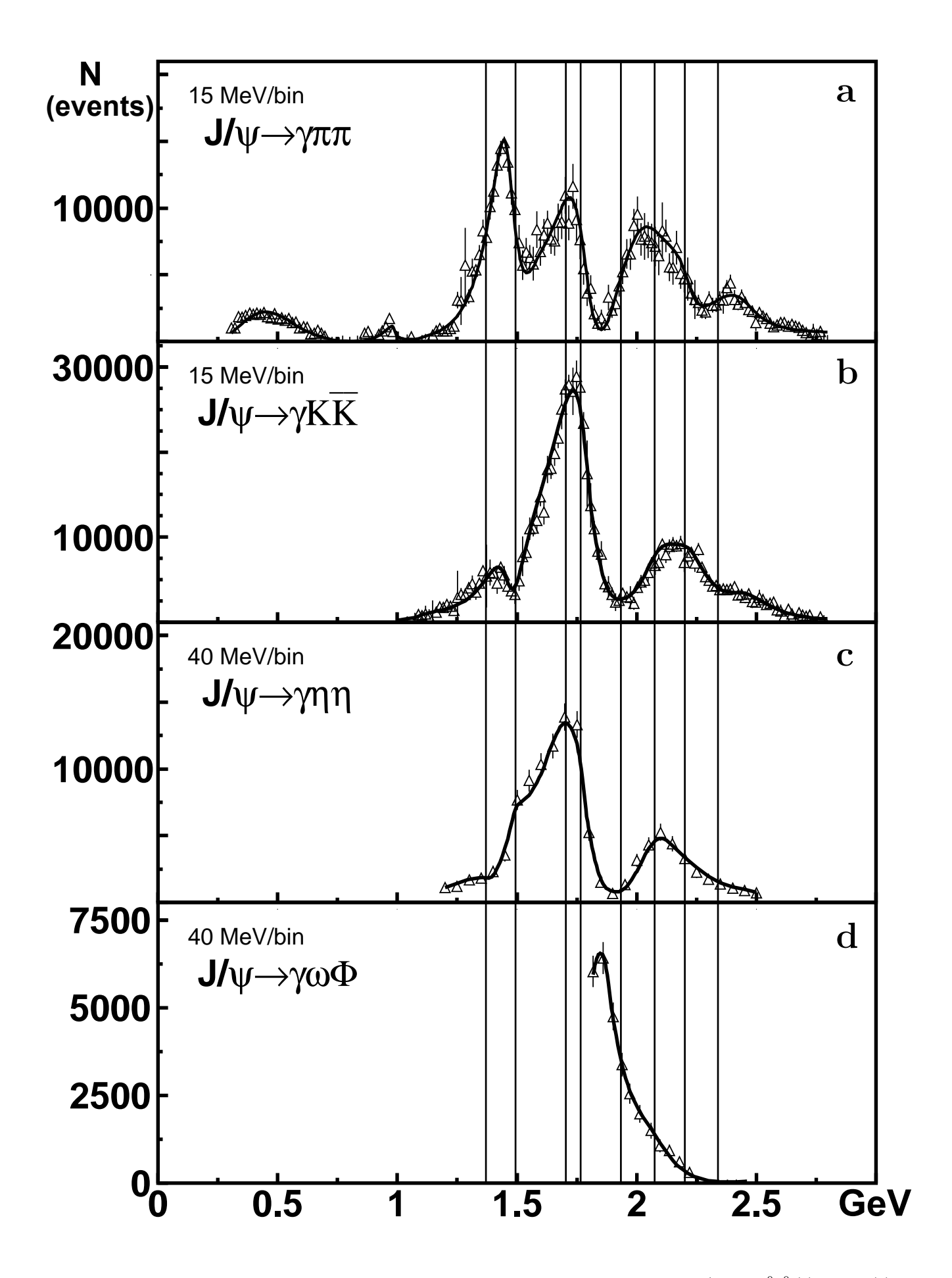


Figure 1: Number of events in the S-wave as functions of the two-meson invariant mass from the reactions $J/\psi \to \gamma \pi^0 \pi^0$ (a), $K_S K_S$ (b), $\eta \eta$ (c), $\phi \omega$ (d). (a) and (b) are based on the analysis of $1.3 \cdot 10^9 \ J/\psi$ decays, (c) and (d) on $0.225 \cdot 10^9 \ J/\psi$ decays.

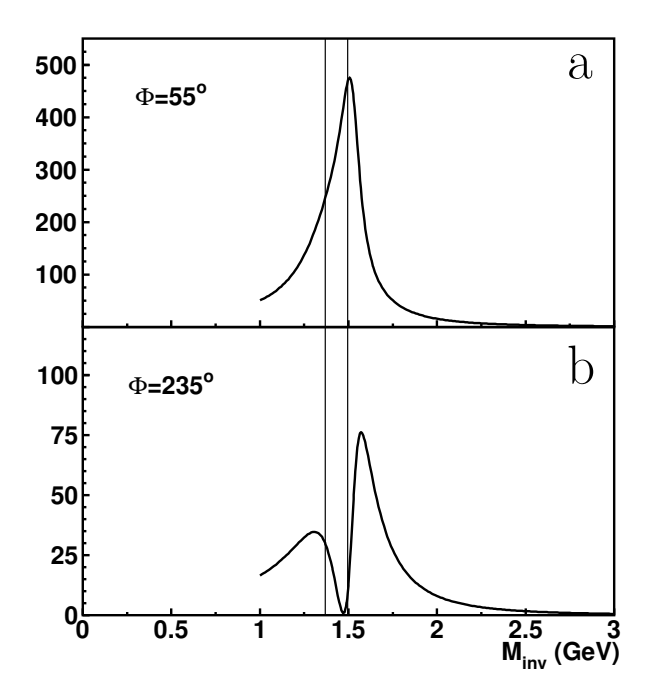


Figure 2: Interference of two K-matrix poles for $f_0(1370)$ and $f_0(1500)$ with a relative phase of 55° (a) and 235° (b). Shown is the intensity in arbitrary units as a function of the two-meson invariant mass.

975 MeV: with $f_0(500)$ and $f_0(980)$. A strong enhancement follows peaking at 1450 MeV, and a second minimum at 1535 MeV. Three more maxima at 1710 MeV. 2000 MeV, and 2400 MeV are separated by a deep minimum at about $1850~\mathrm{MeV}$ and a weak one at $2285~\mathrm{MeV}$. (ii) The K_SK_S invariant mass distribution exhibits a small peak at 1440 MeV immediately followed by a sharp dip at 1500 MeV. The subsequent enhancement - with a peak position of 1730 MeV - has a significant low-mass shoulder. There is a wide minimum at 1940 MeV followed by a further structure peaking at 2160 MeV. It is followed by a valley at 2360 MeV, a small shoulder above 2400 MeV, and a smooth continuation. (iii) Data on $J/\psi \to \gamma \eta \eta$ [21] and $J/\psi \to \gamma \phi \omega$ [22] were published including an interpretation within a partial wave analysis. We extracted the S-wave contributions (Fig. 1c,d) (for [22] only the contribution of the dominant threshold resonance), and included them in the fits. The $\eta\eta$ mass distribution (Fig. 1d) resembles the one observed at SLAC [16], but now greatly improved statistics. The BESIII data show an asymmetry that reveals the presence of at least two resonances, $f_0(1500)$ and $f_0(1710)$. The sharp drop-off above 1.75 GeV indicates destructive interference between two resonances. (iv) The $\phi\omega$ mass distribution exhibits a strong threshold enhancement. It was assigned to a scalar resonance at (1795 ± 7) MeV [22] but the data can also be described by a resonance at 1770 MeV that was suggested earlier [66] and that is required in our fit.

The two figures 1a,b look very different. Obviously, interference between neighboring states plays a decisive role.

Figures 2a,b simulate the observed pattern: in Fig. 2a the low-mass part of $f_0(1500)$ interferes constructively with $f_0(1370)$ and leads to a sharp drop-off at its high-mass part. In Fig. 2b, the $f_0(1500)$ is responsible for the dip. The phase difference between the amplitudes for $f_0(1370)$ and $f_0(1500)$ in figures 2a,b changes by 180° when going from $\pi\pi$ to K_SK_S . This is an important observation: these two states do not behave like a $\frac{1}{\sqrt{2}}(u\bar{u}+d\bar{d})$ and a $s\bar{s}$ state but rather like a singlet and an octet state, like $\frac{1}{\sqrt{3}}(u\bar{u}+d\bar{d}+s\bar{s})$ and $\frac{1}{\sqrt{6}}(u\bar{u}+d\bar{d}-2s\bar{s})$. This change in the sign of the coupling constant in $\pi\pi$ and $K\bar{K}$ decays for $f_0(1500)$ with respect to the $f_0(1370)$ "background" has first been noticed in Ref. [67].

The two resonances $f_0(1710)$ and $f_0(1770)$ form the large enhancement in figure 1b while their contribution to figure 1a is much smaller. This again is due to interference: the two resonances interfere destructively in the $\pi\pi$ channel and constructively in the $K\bar{K}$ channel. Again, the $f_0(1710)$ and $f_0(1770)$ wave functions must contain significant $u\bar{u} + d\bar{d}$ and $s\bar{s}$ contributions of opposite signs: there must one singlet-like and one octet-like state.

3. The PWA

The different sets of partial-wave amplitudes were fitted with a modified K-matrix approach [68] that takes into account dispersive corrections and the Adler zero. We fit data in which resonances are produced and data in which they are formed in scattering processes. The scattering amplitude between the channels a and b is described as

$$A_{ab} = \sum_{\alpha,\beta} g_a^{R(\alpha)} d_{\alpha\alpha} D_{\alpha\beta} g_b^{L(\beta)}, \qquad (1)$$

while the production of a resonance is given by a P-vector amplitude:

$$A_b = \sum_{\alpha,\beta} \tilde{P}^{(\alpha)} d_{\alpha\alpha} D_{\alpha\beta} g_b^{L(\beta)} \quad \tilde{P} = (\Lambda_1, \dots \Lambda_n, F_1, \dots) . \quad (2)$$

The Λ_{α} are production couplings of the resonances, the F_j represent non-resonant transitions from the initial to the final states, and the $g_a^{R(\alpha)}$ and $g_b^{L(\alpha)}$ are right-hand (R) and left-hand (L) coupling constants of the state α into channels a and b. Here the "state" represents either the bare resonant state or a non-resonant contribution. For resonances the vectors of right-hand and left-hand vertices are identical (but transposed), for non-resonant contributions, the vertices can be different, even the sign can differ. The $d_{\alpha\alpha}$ are elements of the diagonal matrix of the propagators \hat{d} :

$$\hat{d} = diag\left(\frac{1}{M_1^2 - s}, \dots, \frac{1}{M_N^2 - s}, R_1, R_2 \dots\right),$$
 (3)

where the first N elements describe propagators of resonances and R_{α} are propagators of non-resonant contributions. Here, these are constants and or a pole well below the $\pi\pi$ threshold.

The block $D_{\alpha\beta}$ describes the transition between the bare state α and the bare state β (with the propagator of the β state included). For this block one can write the equation (with summation over the double indices γ , η)

$$D_{\alpha\beta} = D_{\alpha\gamma} \sum_{j} B_{\gamma\eta}^{j} d_{\eta\beta} + d_{\alpha\beta}. \tag{4}$$

The elements $B_{\gamma\eta}^j$ describe the loop diagrams of the channel j between states γ and η :

$$B_{\alpha\beta}^{j} = \int \frac{ds'}{\pi} \frac{g_j^{R(\alpha)} \rho_j(s', m_{1j}, m_{2j}) g_j^{L(\beta)}}{s' - s - i0} . \tag{5}$$

In matrix form, Eqn. (4) can be written as

$$\hat{D} = \hat{D}\hat{B}\hat{d} + \hat{d}$$
 $\hat{D} = \hat{d}(I - \hat{B}\hat{d})^{-1},$ (6)

where the elements of the $B_{\alpha\beta}$ matrix are equal to the sum of the loop diagrams between states α and β :

$$\hat{B}_{\alpha\beta} = \sum_{j} B_{\alpha\beta}^{j} \ . \tag{7}$$

If only the imaginary part of the integral from Eqn. (5) is taken into account, Eqn. (1) corresponds to the standard K-matrix amplitude. In this case, the energy dependent non-resonant terms can be described by left-hand vertices only, the right-hand vertices can be set to 1.

Here, the real part of the loop diagrams is taken into account, and we parameterize the non-resonant contributions either as constants or as a pole below all relevant thresholds. The latter parameterization reproduces well the projection of the t and u-channel exchange amplitudes into particular partial waves.

The elements of the $B^j_{\alpha\beta}$ are calculated using one subtraction taken at the channel threshold $M_j = (m_{1j} + m_{2j})$:

$$B_{\alpha\beta}^{j}(s) = B_{\alpha\beta}^{j}(M_{j}^{2}) + (s - M_{j}^{2}) \times \int_{M_{i}^{2}}^{\infty} \frac{ds'}{\pi} \frac{g_{j}^{R(\alpha)} \rho_{j}(s', m_{1j}, m_{2j}) g_{j}^{L(\beta)}}{(s' - s - i0)(s' - M_{j}^{2})}.$$
(8)

Our parameterization of the non-resonant contributions allows us to rewrite the \hat{B} matrix as

$$B_{\alpha\beta}^{j}(s) = g_a^{R(\alpha)} \left(b_0^j + (s - M_j^2) b_j(s) \right) g_b^{L(\beta)},$$
 (9)

where the parameters b^{j} depend on decay channels only:

$$b_j(s) = \int_{M_j^2}^{\infty} \frac{ds'}{\pi} \frac{\rho_j(s', m_{1a}, m_{2a})}{(s' - s - i0)(s' - M_j^2)}.$$
 (10)

In this form the D-matrix approach would be equivalent to the K-matrix approach when the substitution

$$i\rho_i(s) \rightarrow b_0^j + (s - M_i^2)b_i(s)$$
 (11)

is made. The Adler zero (set to $s_A=m_\pi^2/2$) is introduced by a modification of the phase volume, with $s_{A_0}{=}0.5\,{\rm GeV^2}$:

$$\rho_1(s, m_\pi, m_\pi) = \frac{s - s_A}{s + s_{A_0}} \sqrt{\frac{s - 4m_\pi^2}{s}}.$$
 (12)

Branching ratios of a resonance into the final state α were determined by defining a Breit-Wigner amplitude in the form

$$A_{\alpha} = \frac{f g_{J/\psi} g_{\alpha}}{M_0^2 - s - i f \sum_{\alpha} g_{\alpha}^2 \rho^{\alpha}(s)}$$
 (13)

The Breit-Wigner mass M_0 and the parameter f are fitted to reproduce the T-matrix pole position. For all states the factor f was between 0.95 and 1.10; the Breit-Wigner mass exceeded the pole mass by 10-20 MeV. The decay couplings g^{α} and production couplings $g_{J/\psi}$ were calculated as residues at the pole position. Then we use the definition (Eqn. (49.16) in [43])

$$M_0 \Gamma^{\alpha} = (g^{\alpha})^2 \rho^{\alpha} (M_0^2); \qquad BR^{\alpha} = \Gamma^{\alpha} / \Gamma_{\text{BW}}.$$
 (14)

Branching ratios into final states with little phase space only were determined by integration over the (distorted) Breit-Wigner function. This procedure is used in publications of the Bonn-Gatchina PWA group and was compared to other definitions in Ref. [69].

The K-matrix had couplings to $\pi\pi$, $K\bar{K}$, $\eta\eta$, $\eta\eta'$, $\phi\omega$, to $\omega\omega$, and to the four-pion phase-space representing unseen multibody final states. The $\omega\omega$ and the four-pion intensities are treated as missing intensity. Fits with K-matrix poles above 1900 MeV were found to be unstable: the CERN-Munich data on elastic scattering and the GAMS data on $\pi\pi \to \pi^0\pi^0$, $\eta\eta$ and $\eta\eta'$ stop at about 1900 MeV. For resonances above, only the product of the coupling constants for production and decay can be determined. Therefore we used K-matrix poles for resonances below and Breit-Wigner amplitudes above 1900 MeV. The latter amplitudes had the form

$$A_{\rm BW} = \frac{g_{\rm BW}}{M_{\rm BW}^2 - s - i M_{\rm BW} \Gamma_{\rm BW}}.$$
 (15)

The total amplitude was thus written as the sum of the *P*-vector amplitude (Eqn. 2) and a summation over for Breit-Wigner amplitudes (Eqn. 15).

Table 1 gives the χ^2 of our best fit for the various data sets. This fit requires contributions from ten resonances. Their masses and widths are given in Table 2, their decay properties in Table 3. The errors stem from the spread of results from different sets of S-wave amplitudes [19, 20], and cover the spread of results when the background amplitude was altered (constant transition amplitudes or lefthand pole in the K matrix), when the number of high-mass resonances was changed (between 7 and 11), and part of the data were excluded from the fit. The resulting values are compared to values listed in the RPP [43]. The overall agreement is rather good. Only the five low-mass resonances are classified as established in the RPP, the other states needed confirmation. We emphasize that the solution presented here was developed step by step, independent from the RPP results. The comparison was made only when the manuscript was drafted.

The sum of Breit-Wigner amplitudes is not manifestly unitary. However, radiative J/ψ decays and the two-body

Table 1: $\chi^2/N_{\rm data}$ contribution from radiative J/ψ decays, charge exchange reactions, $K_{\rm e4}$ decays, and Dalitz plots from $\bar{p}N$ annihilation at rest. Dalitz plots are given by the number of events in cells, N is the number of cells.

$J/\Psi \rightarrow$	χ^2/N	N	Ref.	$\bar{p}p(liq) \rightarrow$	χ^2/N	N	Ref.
$\gamma \pi^0 \pi^0$	1.28	167	[19]	$\pi^0\pi^0\pi^0$	1.40	7110	[26]
$\gamma K_S K_S$	1.21	121	[20]	$\pi^0\eta\eta$	1.28	3595	[27]
$\gamma\eta\eta$	0.80	21	[21]	$\pi^0\pi^0\eta$	1.23	3475	[59]
$\gamma\phi\omega$	0.2	17	[22]	$\pi^{+}\pi^{0}\pi^{-}$	1.24	1334	[60]
$\pi^-\pi^+ \rightarrow$				$K_L K_L \pi^0$	1.08	394	[29]
$\pi^0\pi^0$	0.89	110	[38]	$K^{+}K^{-}\pi^{0}$	0.97	521	[61]
$\eta\eta$	0.67	15	[38]	$K_S K^{\pm} \pi^{\mp}$	2.13	771	[62]
$\eta\eta'$	0.23	9	[38]	$K_L K^{\pm} \pi^{\mp}$	0.76	737	[63]
K^+K^-	1.06	35	[40]	$\bar{p}n(liq) \rightarrow$			
$\pi^+\pi^-$	1.32	845	[41]	$\pi^{+}\pi^{-}\pi^{-}$	1.39	823	[58]
$\delta(elastic)$	0.91	17	[42]	$\pi^0 \pi^0 \pi^-$	1.57	825	[60]
$\bar{p}p(gas) \rightarrow$				$K_SK^-\pi^0$	1.33	378	[62]
$\pi^0\pi^0\pi^0$	1.36	4891	[57]	$K_SK_S\pi^-$	1.62	396	[62]
$\pi^0\eta\eta$	1.32	1182	[57]				
$\pi^0\pi^0\eta$	1.24	3631	[58]				

decays of high-mass resonances are far from the unitarity limit. To check possible systematic errors due to the use of Breit-Wigner amplitudes, we replace the four resonances $f_0(1370)$, $f_0(1500)$, $f_0(1710)$, $f_0(1770)$ by Breit-Wigner amplitudes (imposing mass and width of $f_0(1370)$). The fit return properties of these resonances within the errors quoted in the Table 2 and 3.

The four lower-mass resonances, one scalar state at about 1750 MeV and the $f_0(2100)$, are mandatory for the fit: if one of them is excluded, no acceptable description of the data is obtained. Only one state, $f_0(1770)$, is "new". Based on different peak positions, Bugg [66] had suggested that $f_0(1710)$ should have a close-by state called $f_0(1770)$. When $f_0(1710)$ and $f_0(1770)$ are replaced by one resonance, the $\chi^2/N_{\rm data}$ increases by 58/167 for $J/\psi \to \gamma \pi \pi$, 8/121 for $J/\psi \to \gamma K\bar{K}$, 50/21 for $J/\psi \to \gamma \eta \eta$, or by (58, 8, 50) in short. When $f_0(2020)$, $f_0(2200)$, or $f_0(2330)$ are removed, the χ^2 increases by (48, 6, 5); (30,6,1); (23, 5, 0). In addition, there is a very significant deterioration of the fit to the Dalitz plots for $\bar{p}p$ annihilation when only one scalar resonance in the 1700 to 1800 MeV range is admitted. When high-mass poles are removed, a small change in χ^2 is observed also in the data on $\bar{p}p$ annihilation due to a change of the interference between neighboring poles. All ten states contribute to the reactions studied here.

4. The flavor wave functions

The interference pattern in Fig. 1a,b suggests that the two pairs of resonances, $f_0(1370)$ - $f_0(1500)$ and $f_0(1710)$ - $f_0(1770)$, have wave flavor functions in which the $u\bar{u}+d\bar{d}$ and $s\bar{s}$ components have opposite signs. Vector (ω,ϕ) and tensor $(f_2(1270),f_2'(1525))$ mesons show ideal mixing, with approximately $1/\sqrt{2}(u\bar{u}+d\bar{d})$ and $s\bar{s}$ configurations. (We

neglect the small mixing angles in this discussion.) The mass difference is 200 to 250 MeV, and the $s\bar{s}$ mesons decay preferably into $K\bar{K}$. This is not the case for the scalar mesons: The mass difference varies, and the $K\bar{K}/\pi\pi$ decay ratio is often less than 1 and never \sim 100 like for $f_2'(1525)$. The decay pattern rules out the possibility that the scalar resonances are states with a dominant $s\bar{s}$ component.

Pseudoscalar mesons are different: the isoscalar mesons are better approximated by SU(3) singlet and octet configurations. Pseudoscalar mesons have both, $1/\sqrt{2}(u\bar{u}+d\bar{d})$ and $s\bar{s}$ components as evidenced by the comparable rates for $J/\psi \to \eta\omega, \eta\phi, \eta'\omega, \eta'\phi$.

In view of these arguments and the interference pattern discussed above, we make a very simple assumption: we assume that the upper states in Table 2 all have large SU(3)-singlet components, while the lower states have large octet components. For the two lowest-mass mesons, $f_0(500)$ and $f_0(980)$, Oller [70] determined the mixing angle to be small, $(19\pm5)^{\circ}$: $f_0(500)$ is dominantly SU(3) singlet, $f_0(980)$ mainly octet.

We choose $f_0(1500)$ as reference state and plot a (M^2, n) trajectory with $M_n^2 = 1.483^2 + n \, a \, \text{GeV}^2, n = -1, 0, 1, \cdots$, where a = 1.08 is the slope of the trajectory. States close to this trajectory are assumed to be mainly SU(3) octet states. In instanton-induced interactions, the separation in mass square of scalar singlet and octet mesons is the same as the one for pseudoscalar mesons, but reversed [71]. Hence we calculate a second trajectory $m_n^2 = 1.483^2 + m_\eta^2 - m_{\eta'}^2 + n \, a \, \text{GeV}^2, n = -1, 0, 1, \cdots$. The low-mass singlet mesons are considerably wider than their octet partners. With increasing mass, the width of singlet mesons become smaller (except for $f_0(2020)$), those of octet mesons increase (except for $f_0(2330)$).

Figure 3 shows (M^2, n) trajectories for "mainly-octet" and "mainly-singlet" resonances. The agreement is not perfect but astonishing for a two-parameter prediction. The interpretation neglects singlet-octet mixing; there could be tetraquark, meson-meson or glueball components that can depend on n; final-state interactions are neglected; close-by states with the same decay modes repel each other. There is certainly a sufficient number of reasons that may distort the scalar-meson mass spectrum. In spite of this, the mass of none of the observed states is incompatible with the linear trajectory by more than its half-width.

Now we comment on the $\phi\omega$ decay mode. The prominent peak in Fig. 1d is ascribed to $f_0(1770) \to \phi\omega$ decays. The BESIII collaboration interpreted the reaction as doubly OZI suppressed decay [22]. We assume that all scalar mesons have a tetraquark component as suggested by Jaffe [4] for the light scalar meson-nonet: the price in energy to excite a $q\bar{q}$ pair to orbital angular momentum L=1 (to 3P_0) is similar to the energy required to create a new $q\bar{q}$ pair with all four quarks in the S-state. Thus, a tetraquark component in scalar mesons should not be surprising. The tetraquark component may decay to two mesons by rearrangement of color; thus a small tetraquark component could have a significant impact on the decays.

Table 2: Pole masses and widths (in MeV) of scalar mesons. The RPP values are listed as small numbers for comparison.

Name	$f_0(500)$	$f_0(1370)$	$f_0(1710)$	$f_0(2020)$	$f_0(2200)$
$M \; [\mathrm{MeV}]$	410 ± 20 $400\rightarrow550$	1370 ± 40 $1200\rightarrow1500$	1700 ± 18 1704 ± 12	1925 ± 25 1992 ± 16	2200 ± 25 2187 ± 14
$\Gamma \ [{ m GeV}]$	480 ± 30 $400\rightarrow700$	390 ± 40 $100\rightarrow500$	255 ± 25 123 ± 18	320 ± 35 442 ± 60	150 ± 30 ~ 200
Name	$f_0(980)$	$f_0(1500)$	$f_0(1770)$	$f_0(2100)$	$f_0(2330)$
$M [\mathrm{GeV}]$	1014±8 990±20	1483 ± 15 1506 ± 6	1765±15	$2075\pm20 \\ 2086^{+20}_{-24}$	2340±20 ~2330
$\Gamma \ [{ m MeV}]$	71 ± 10 $_{10\rightarrow100}$	$116{\pm}12\atop_{112{\pm}9}$	180±20	$260 \pm 25 \\ 284^{+60}_{-32}$	$165{\pm}25_{250{\pm}20}$

Table 3: J/ψ radiative decay rates in 10^{-5} units. Small numbers represent the RPP values, except the 4π decay modes that gives our estimates derived from [23, 24]. The RPP values and those from Refs. [23, 24] are given with small numbers and with two digits only; statistical and systematic errors are added quadratically. The missing intensities in parentheses are our estimates. Ratios for $K\bar{K}$ are calculated from K_SK_S by multiplication with a factor 4. Under $f_0(1750)$ we quote results listed in RPP as decays of $f_0(1710)$, $f_0(1750)$ and $f_0(1800)$. The RPP values should be compared to the sum of our yields for $f_0(1710)$ and $f_0(1770)$. BES [20] uses two scalar resonances, $f_0(1710)$ and $f_0(1790)$ and assigns most of the $K\bar{K}$ intensity to $f_0(1710)$. Likewise, the yield of three states at higher mass should be compared to the RPP values for $f_0(2100)$ or $f_0(2200)$.

$BR_{J/\psi \to \gamma f_0 \to}$	$\gamma\pi\pi$	$\gamma K ar{K}$	$\gamma\eta\eta$	$\gamma\eta\eta'$	$\gamma \omega \phi$		total	unit
$f_0(500)$	105±20	5±5	4±3	~0	~0	~0	114±21	$\otimes 10^{-5}$
$f_0(980)$	1.3 ± 0.2	$0.8 {\pm} 0.3$	~ 0	~ 0	~ 0	~0	2.1±0.4	$\otimes 10^{-5}$
$f_0(1370)$	38±10	13 ± 4 42 ± 15	3.5 ± 1	0.9 ± 0.3	~0	14 ± 5 27 ± 9	69±12	$\otimes 10^{-5}$
$f_0(1500)$	$9.0 {\pm} 1.7$	3 ± 1	1.1 ± 0.4	$1.2 {\pm} 0.5$	~ 0	33 ± 8	47±9	$\otimes 10^{-5}$
	10.9 ± 2.4	$2.9 {\pm} 1.2$	$1.7^{+0.6}_{-1.4}$	$6.4^{+1.0}_{-2.2}$		36±9		⊗10 °
$f_0(1710)$	6 ± 2	23 ± 8	12 ± 4	$6.5 {\pm} 2.5$	1 ± 1	7 ± 3	56±10	
$f_0(1770)$	24 ± 8	60 ± 20	7 ± 1	$2.5{\pm}1.1$	22 ± 4	65 ± 15	181±26	$\otimes 10^{-5}$
$f_0(1750)$	38±5	99^{+10}_{-6}	24^{+12}_{-7}		25 ± 6	97 ± 18 31 ± 10		
$f_0(2020)$	42 ± 10	55 ± 25	10 ± 10			(38±13)	145±32	
$f_0(2100)$	20 ± 8	32 ± 20	18 ± 15			(38 ± 13)	108±25	$\otimes 10^{-5}$
$f_0(2200)$	5 ± 2	5 ± 5	$0.7 {\pm} 0.4$			(38 ± 13)	49±17	\otimes 10
$f_0(2100)/f_0(2200)$	62 ± 10	$109^{+\ 8}_{-19}$	$11.0_{-3.0}^{+6.5}$			115±41		
$f_0(2330)$	4 ± 2	2.5 ± 0.5 $_{20\pm3}$	1.5 ± 0.4				8±3	$\otimes 10^{-5}$

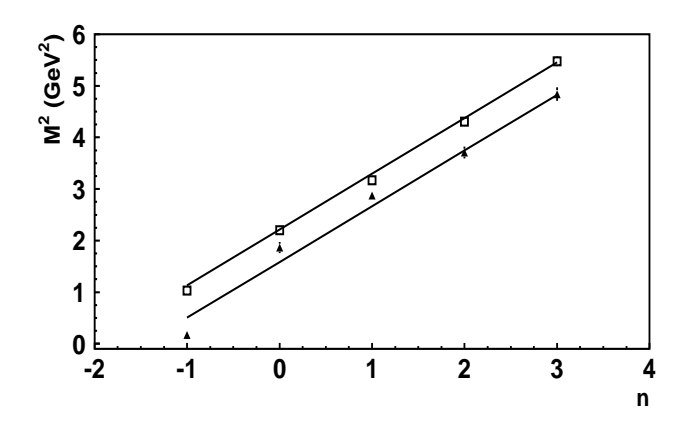


Figure 3: Squared masses of mainly-octet and mainly-singlet scalar isoscalar mesons as functions of a consecutive number.

The ϕ and ω are orthogonal in SU(3), thus $f_0(1770)$ must have a large octet component. The $\phi\omega$ decay is assigned to the $\frac{1}{\sqrt{6}}(2u\bar{u}d\bar{d}-u\bar{u}s\bar{s}-d\bar{d}s\bar{s})$ component that can easily disintegrate into $\phi\omega$. Scalar SU(3) singlet mesons might have a $\frac{1}{\sqrt{3}}(u\bar{u}d\bar{d}+u\bar{u}s\bar{s}+d\bar{d}s\bar{s})$ component but their coupling to $\phi\omega$ is small since these two mesons cannot come from a pure SU(3) singlet state. The ϕ and ω are orthogonal in SU(3), thus $f_0(1770)$ must have a large octet component. The $\phi\omega$ decay is assigned to the $\frac{1}{\sqrt{6}}(2u\bar{u}d\bar{d}-u\bar{u}s\bar{s}-d\bar{d}s\bar{s})$ component that can easily disintegrate into $\phi\omega$. Scalar SU(3) singlet mesons might have a $\frac{1}{\sqrt{3}}(u\bar{u}d\bar{d}+u\bar{u}s\bar{s}+d\bar{d}s\bar{s})$ component but their coupling to $\phi\omega$ is small since these two mesons cannot come from a pure SU(3) singlet state.

5. Multiparticle decays

Scalar mesons may also decay into multi-meson final states. This fraction is determined here as missing intensity in the mass range where data on $\pi-\pi$ elastic scattering are available. The results are also given in Table 3 and compared to earlier determinations. The reaction $J/\psi \to \gamma \pi^+ \pi^- \pi^+ \pi^-$ has been studied in Refs. [23, 24]. The partial wave analyses determined $\sigma\sigma$ as main decay mode of the scalar mesons. Then, the yields seen in $2\pi^+ 2\pi^-$ need to be multiplied by 9/4 to get the full four-pion yield. These estimated yields for $J/\psi \to \gamma 4\pi$ are given in Table 3 by small numbers. Assuming different decay modes (like those reported in Table III in [33]) leads to small changes only in the four-pion yields. The $\omega\omega$ yield, determined in $J/\psi \to \gamma\omega\omega$ [25], is unexpectedly large and inconsistent with the small $\rho^0\rho^0$ yield.

The missing intensity of $f_0(1370)$ reported here is not inconsistent with the branching ratio found in radiative decays $J/\psi \to \gamma \pi^+ \pi^- \pi^+ \pi^-$ but contradicts the findings from $\bar{p}N$ annihilation into five pions and from central production of four pions. This discrepancy can only be resolved by analyzing data on $J/\psi \to \gamma 4\pi$ and $\bar{p}N$ annihilation in a coupled-channel analysis. The inclusion of both

data sets seems to be of particular importance.

Not all scalar resonances found here were identified in $J/\psi \to \gamma 4\pi$ [23, 24] and $J/\psi \to \gamma \omega \omega$ [25]. Therefore we compare our missing intensities for $f_0(1710)$ and $f_0(1770)$ with the measured 4π and the $\omega\omega$ decay modes assigned to $f_0(1750)$. Our missing intensities are mostly well compatible with the measured 4π and 2ω yields. For the high-mass states we distribute the measured 4π intensity among the three resonances with masses close to the $f_0(2100)$. Our estimated intensities are given in Table 3 in parentheses. Changing how the 4π intensity is distributed has little effect on the properties of the peak shown in Fig. 4.

6. The integrated yield

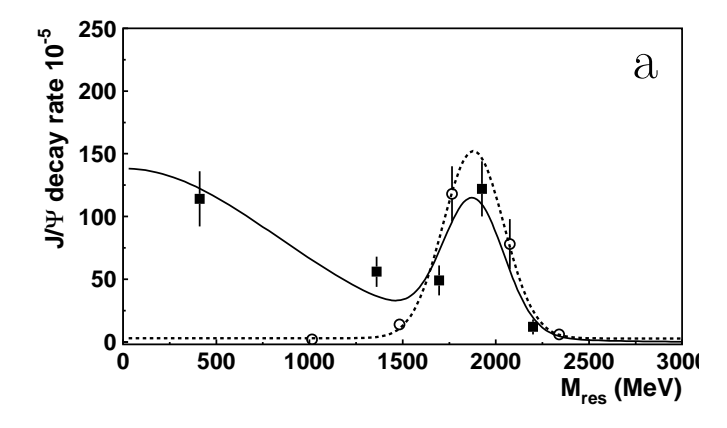
Figure 4 shows the yields of scalar SU(3)-singlet and octet resonances as functions of their mass, for two-body decays in Fig. 4a and for all decay modes (except 6π) in Fig. 4b. SU(3)-octet mesons are produced in a limited mass range only. In this mass range, a clear peak shows up. SU(3)-singlet mesons are produced over the full mass range but at about 1900 MeV, their yield is enhanced. Obviously, the two gluons from radiative J/ψ decays couple to SU(3) singlet mesons in the full mass range while octet mesons are formed only in a very limited mass range. But both, octet and singlet scalar isoscalar mesons are formed preferentially in the 1700 to 2100 MeV mass range.

The peak structure is unlikely to be explained as kinematics effect. Billoire et al. [72] have calculated the mass spectrum of two gluons produced in radiative J/ψ decay. For scalar quantum numbers, the distribution has a maximum at about 2100 MeV and goes down smoothly in both directions. Körner et al. [73] calculated the (squared) amplitude to produce scalar mesons in radiative J/ψ decays. The smooth amplitude does not show any peak structure, neither.

7. The scalar glueball

We suggest to interpret this enhancement as the scalar glueball of lowest mass. The scalar isoscalar mesons that we assigned to the SU(3) octet seem to be produced only via their mixing with the glueball. Indeed, $J/\psi \to \gamma f_0^8$ decays are expected to be suppressed: two gluons cannot couple to one SU(3) octet meson. Mesons interpreted as singlet scalar isoscalar mesons are produced over the full mass range. This finding supports strongly the interpretation of the scalar mesons as belonging to SU(3) singlet and octet.

Figure 4a and 4b are fitted with a Breit-Wigner amplitude. We determined the yield of the scalar glueball as sum of the yield of "octet" scalar mesons plus the yield of "singlet" scalar mesons above a suitably chosen phenomenological background. Different background shapes were assumed. Shown is a background of the form $x \cdot \exp\{-\alpha M^2\}$ $(x = 149, \alpha = 0.73/\text{GeV}^2)$. For Fig. 4a, we find $(M, \Gamma) = 0.73/\text{GeV}^2$



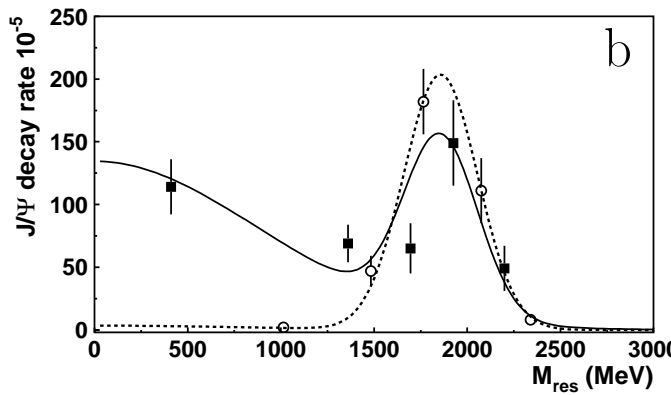


Figure 4: (color online) Yield of radiatively produced scalar isoscalar octet mesons (open circles) and singlet (full squares) mesons. a) Yield for $\pi\pi$, $K\bar{K}$, $\eta\eta$, $\eta\eta'$, and $\phi\omega$ decays. b) Yield when 4π decays and $\omega\omega$ are included.

 $(1872,332)\,\mathrm{MeV}$, for Fig. 4b $(M,\Gamma)=(1856,396)\,\mathrm{MeV}$. The results depend on the background chosen. From the spread of results when the background function is changed, we estimate the uncertainty. Our best estimate for the scalar glueball mass and width is given as

$$M_G = (1865 \pm 25^{+10}_{-30}) \,\text{MeV} \quad \Gamma_G = (370 \pm 50^{+30}_{-20}) \,\text{MeV}.$$

The integrated yields depend on the not well-known 4π and $\omega\omega$ (and unknown 6π) contributions. The (observed) yield of octet scalar isoscalar mesons plus the yield of singlet mesons above the background is determined to

$$Y_{J/\psi \to \gamma G} = (5.8 \pm 1.0) \, 10^{-3}.$$

The two states with the largest glueball component are $f_0(1770)$ and $f_0(2020)$. The "mainly octet" $f_0(1770)$ acquires a glueball component (and is no longer "mainly octet", only the $q\bar{q}$ and tetraquarks components belong to the octet). We suggest their wave functions could contain a small $q\bar{q}$ component (a $q\bar{q}$ seed), a small tetraquark component as discussed above, and a large glueball component. At the present statistical level, there seem to be no direct decays of the glueball to mesons; the two gluons forming a glueball are seen only since the glueball mixes with scalar mesons. We observe no "extra" state.

8. Summary

Summarizing, we have performed a first coupled-channel analysis of the S-wave partial-wave amplitudes for J/ψ radiative decays into $\pi\pi$, K_SK_S , $\eta\eta$, and $\phi\omega$ decays. The fits were constrained by a large number of further data. The observed pattern of peaks and valleys in the $\pi\pi$ and $K\bar{K}$ invariant mass distributions depends critically on the interference between neighboring states. We are convinced that only a coupled-channel analysis has the sensitivity to identify reliably the position of resonances.

Scalar mesons seem to show up as mainly-singlet and mainly-octet states in SU(3). The masses of both, of singlet and octet states, are compatible with a linear (M^2, n)

behavior. Only the $f_0(500)$, mostly interpreted as dynamically generated $\pi\pi$ molecule, does not fall onto the trajectory. The $\omega\phi$ decay mode of some scalar resonances suggests that these may have a tetraquark component as it was suggested for the lowest-mass scalar-meson nonet by Jaffe 45 years ago. Thus, a simple picture of the scalar-meson mass spectrum has emerged. The yield of scalar mesons in radiative J/ψ decays shows a significant structure that we propose to interpret as scalar glueball.

The BESIII collaboration has recorded data with significantly improved quality and statistics. It seems very important to repeat this analysis with the full statistics and including all final states into which scalar mesons can decay.

Acknowledgement

Funded by the NSFC and the Deutsche Forschungsgemeinschaft (DFG, German Research Foundation) through the funds provided to the Sino-German Collaborative Research Center TRR110 "Symmetries and the Emergence of Structure in QCD" (NSFC Grant No. 12070131001, DFG Project-ID 196253076 - TRR 110) and the Russian Science Foundation (RSF 16-12-10267).

References

- Y. Nambu, "Axial vector current conservation in weak interactions," Phys. Rev. Lett. 4, 380 (1960).
- [2] Y. Nambu, "Nobel Lecture: Spontaneous symmetry breaking in particle physics: A case of cross fertilization," Rev. Mod. Phys. 81, 1015 (2009).
- [3] J. R. Pelaez, "On the Nature of light scalar mesons from their large N_c behavior," Phys. Rev. Lett. **92**, 102001 (2004) .
- [4] R. L. Jaffe, "Multi-Quark Hadrons. 1. The Phenomenology of $(2Q2\bar{Q})$ Mesons," Phys. Rev. D **15**, 267 (1977).
- [5] H. Fritzsch and M. Gell-Mann, "Current algebra: Quarks and what else?," eConf C720906V2, 135 (1972).
- [6] H. Fritzsch and P. Minkowski, "Psi Resonances, Gluons and the Zweig Rule," Nuovo Cim. A 30, 393 (1975).

- [7] T. A. DeGrand, R. L. Jaffe, K. Johnson and J. E. Kiskis, "Masses and Other Parameters of the Light Hadrons," Phys. Rev. D 12 (1975), 2060.
- [8] G. S. Bali et al. [UKQCD Collaboration], "A Comprehensive lattice study of SU(3) glueballs," Phys. Lett. B 309, 378 (1993).
- [9] C. J. Morningstar and M. J. Peardon, "The Glueball spectrum from an anisotropic lattice study," Phys. Rev. D 60, 034509 (1999).
- [10] A. Athenodorou and M. Teper, "The glueball spectrum of SU(3) gauge theory in 3 + 1 dimensions," JHEP 11, 172 (2020).
- [11] E. Gregory, A. Irving, B. Lucini, C. McNeile, A. Rago, C. Richards and E. Rinal- di, "Towards the glueball spectrum from unquenched lattice QCD," JHEP 1210, 170 (2012).
- [12] A. P. Szczepaniak and E. S. Swanson, "The low lying glueball spectrum," Phys. Lett. B 577, 61-66 (2003).
- [13] M. Q. Huber, C. S. Fischer and H. Sanchis-Alepuz, "Spectrum of scalar and pseudoscalar glueballs from functional methods," Eur. Phys. J. C 80 no.11, 1077 (2020).
- [14] M. Rinaldi and V. Vento, "Meson and glueball spectroscopy within the graviton soft wall model," [arXiv:2101.02616 [hepph]].
- [15] L. C. Gui et al. [CLQCD], "Scalar Glueball in Radiative J/ψ Decay on the Lattice," Phys. Rev. Lett. 110 no.2, 021601 (2013).
- [16] C. Edwards et al., "Observation of an $\eta\eta$ Resonance in J/ψ Radiative Decays," Phys. Rev. Lett. 48, 458 (1982).
- [17] J. E. Augustin *et_al.* [DM2], "Measurement of the Radiative J/ψ Decays in $K\bar{K}$ States," Phys. Rev. Lett. **60**, 2238 (1988).
- [18] S. Dobbs, A. Tomaradze, T. Xiao and K. K. Seth, "Comprehensive Study of the Radiative Decays of J/ψ and $\psi(2S)$ to Pseudoscalar Meson Pairs, and Search for Glueballs," Phys. Rev. D **91**, no.5, 052006 (2015).
- [19] M. Ablikim et al. [BESIII Collaboration], "Amplitude analysis of the $\pi^0\pi^0$ system produced in radiative J/ψ decays," Phys. Rev. D **92** no.5, 052003 (2015).
- [20] M. Ablikim et al. [BESIII Collaboration], "Amplitude analysis of the K_SK_S system produced in radiative J/ψ decays," Phys. Rev. D **98** no.7, 072003 (2018).
- [21] M. Ablikim *et al.* [BESIII Collaboration], "Partial wave analysis of $J/\psi \to \gamma \eta \eta$," Phys. Rev. D **87**, no. 9, 092009 (2013).
- [22] M. Ablikim et al. [[BESIII Collaboration], "Study of the nearthreshold $\omega\phi$ mass enhancement in doubly OZI-suppressed $J/\psi \to \gamma\omega\phi$ decays," Phys. Rev. D 87 no.3, 032008 (2013).
- [23] J. Z. Bai et al. [BES], "Partial wave analysis of $J/\psi \to \gamma(\pi^+\pi^-\pi^+\pi^-)$," Phys. Lett. B **472**, 207 (2000).
- [24] D. V. Bugg, "Study of $J/\psi \to \gamma \pi^+ \pi^- \pi^+ \pi^-$," (unpublished) [arXiv:0907.3021 [hep-ex]].
- [25] M. Ablikim et al. [BES Collaboration], "Pseudoscalar production at $\omega\omega$ threshold in $J/\psi \to \gamma\omega\omega$," Phys. Rev. D **73**, 112007 (2006).
- [26] C. Amsler *et al.* [Crystal Barrel Collaboration], "High statistics study of $f_0(1500)$ decay into $\pi^0\pi^0$," Phys. Lett. B **342**, 433 (1995).
- [27] C. Amsler *et al.* [Crystal Barrel Collaboration], "High statistics study of $f_0(1500)$ decay into $\eta\eta$," Phys. Lett. B **353**, 571 (1995).
- [28] C. Amsler *et al.* [Crystal Barrel Collaboration], " $\eta\eta'$ threshold enhancement in $\bar{p}p$ annihilations into $\pi^0\eta\eta'$ at rest," Phys. Lett. B **340**, 259 (1994).
- [29] A. Abele *et al.* [Crystal Barrel Collaboration], "Observation of $f_0(1500)$ decay into K_LK_L ," Phys. Lett. B **385**, 425 (1996).
- [30] A. Bettini, M. Cresti, S. Limentani, L. Bertanza and A. Bigi, "Evidence for Strong, Possibly Resonant, Scalar ρρ Interaction," Nuovo Cim. A 42, 695 (1966).
- [31] C. Amsler et al. [Crystal Barrel Collaboration], "Observation of a scalar resonance decaying to $\pi^+\pi^-\pi^0\pi^0$ in $\bar{p}p$ annihilation at rest," Phys. Lett. B **322**, 431 (1994).
- [32] A. Abele et al. [Crystal Barrel Collaboration], "Study of f₀ decays into four neutral pions," Eur. Phys. J. C 19, 667 (2001).
- [33] A. Abele *et al.* [Crystal Barrel Collaboration], "4π decays of scalar and vector mesons," Eur. Phys. J. C **21**, 261 (2001).
- [34] D. Barberis *et al.* [WA102 Collaboration], "A Coupled channel analysis of the centrally produced K^+K^- and $\pi^+\pi^-$ final states

- in pp interactions at 450 GeV/c," Phys. Lett. B **462**, 462 (1999).
- [35] D. Barberis *et al.* [WA102 Collaboration], "A Study of the $\eta\eta$ channel produced in central pp interactions at 450 GeV/c," Phys. Lett. B **479**, 59 (2000).
- [36] D. Barberis *et al.* [WA102 Collaboration], "A Study of the $\eta\eta'$ and $\eta'\eta'$ channels produced in central pp interactions at 450 GeV/c," Phys. Lett. B **471**, 429 (2000).
- [37] D. Barberis *et al.* [WA102 Collaboration], "A Study of the $f_0(1370)$, $f_0(1500)$, $f_0(2000)$ and $f_2(1950)$ observed in the centrally produced 4π final states," Phys. Lett. B **474**, 423 (2000).
- [38] D. Alde *et al.* [GAMS Collaboration], "Study of the $\pi^0\pi^0$ system with the GAMS-4000 spectrometer at 100 GeV/c," Eur. Phys. J. A **3**, 361 (1998).
- [39] R. S. Longacre *et al.*, "A Measurement of $\pi^-p \to K_S K_S n$ at 22 GeV/c and a Systematic Study of the 2⁺⁺ Meson Spectrum," Phys. Lett. B **177**, 223 (1986).
- [40] S. J. Lindenbaum and R. S. Longacre, "Coupled channel analysis of $J^{PC}=0^{++}$ and 2^{++} isoscalar mesons with masses below 2 GeV," Phys. Lett. B **274**, 492 (1992).
- [41] G. Grayer *et al.*, "High Statistics Study of the Reaction $\pi^- p \to \pi^- \pi^+ n$: Apparatus, Method of Analysis, and General Features of Results at 17 GeV/c," Nucl. Phys. B **75**, 189 (1974).
- [42] J. R. Batley *et al.* [NA48/2 Collaboration], "Precise tests of low energy QCD from K_{e4} decay properties," Eur. Phys. J. C **70** 635 (2010).
- [43] P. A. Zyla et al. [Particle Data Group], "Review of Particle Physics," PTEP 2020 083C01 (2020).
- [44] C. Amsler and F. E. Close, "Evidence for a scalar glueball," Phys. Lett. B 353, 385 (1995).
- [45] C. Amsler and F. E. Close, "Is $f_0(1500)$ a scalar glueball?," Phys. Rev. D **53**, 295 (1996).
- [46] X. Guo, H. Ke, M. Zhao, L. Tang and X. Li, "Revisiting the topic of determining fraction of glueball component in f₀ mesons via radiative decays of J/\(\psi\)," [arXiv:2003.07116 [hep-ph]].
- [47] E. Klempt and A. Zaitsev, "Glueballs, Hybrids, Multiquarks. Experimental facts versus QCD inspired concepts," Phys. Rept. 454, 1 (2007).
- [48] W. Ochs, "Spectroscopy with glueballs and the role of $f_0(1370)$," Acta Phys. Polon. Supp. **6**, no. 3, 839 (2013).
- [49] P. Minkowski and W. Ochs, "Identification of the glueballs and the scalar meson nonet of lowest mass," Eur. Phys. J. C 9, 283 (1999).
- [50] A. V. Anisovich, V. V. Anisovich and A. V. Sarantsev, "0⁺⁺ glueball / $q\bar{q}$ state mixing in the mass region near 1500 MeV," Phys. Lett. B **395**, 123 (1997).
- [51] A. V. Anisovich, V. V. Anisovich and A. V. Sarantsev, "Scalar glueball: Analysis of the $(IJ^{PC}=00^{++})$ wave," Z. Phys. A **359**, 173 (1997).
- [52] D. V. Bugg, M. J. Peardon and B. S. Zou, "The Glueball spectrum," Phys. Lett. B 486, 49 (2000).
- [53] V. Mathieu, N. Kochelev and V. Vento, "The Physics of Glueballs," Int. J. Mod. Phys. E 18, 1 (2009).
- [54] V. Crede and C. A. Meyer, "The Experimental Status of Glueballs," Prog. Part. Nucl. Phys. 63, 74 (2009).
- [55] W. Ochs, "The Status of Glueballs," J. Phys. G 40, 043001 (2013).
- [56] F. J. Llanes-Estrada, "Glueballs as the Ithaca of meson spectroscopy," [arXiv:2101.05366 [hep-ph]].
- [57] C. Amsler et al. [Crystal Barrel Collaboration], "Annihilation at rest of antiprotons and protons into neutral particles," Nucl. Phys. A 720, 357 (2003).
- [58] A. Abele *et al.* [Crystal Barrel Collaboration], "Evidence for a $\pi\eta$ P-wave in $\bar{p}p$ annihilations at rest into $\pi^0\pi^0\eta$," Phys. Lett. B **446**, 349 (1999).
- [59] C. Amsler *et al.* [Crystal Barrel Collaboration], "Observation of a new $I^G(J^{PC})=1^-(O^{++})$ resonance at 1450 MeV," Phys. Lett. B **333**, 277 (1994).
- [60] A. Abele *et al.* [Crystal Barrel Collaboration], "High mass ρ meson states from $\bar{p}d$ annihilation at rest into $\pi^-\pi^0\pi^0$ spectator," Phys. Lett. B **391**, 191 (1997).
- [61] A. Abele et al. [Crystal Barrel Collaboration], "Anti-proton pro-

- ton annihilation at rest into $K^+K^-\pi^0$," Phys. Lett. B **468**, 178 (1999).
- [62] K. Wittmack, "Messung der Reaktionen $\bar{p}n \to K_S K^- \pi^0$ and $\bar{p}n \to K_S K_S \pi^-$ ", PhD thesis, Bonn (2001).
- [63] A. Abele *et al.* [Crystal Barrel Collaboration], $\bar{p}p$ annihilation at rest into $K_LK^{\pm}\pi^{\mp}$ Phys. Rev. D **57**, 3860 (1998).
- [64] A. Abele *et al.* [Crystal Barrel Collaboration], "The ρ mass, width and line-shape in $p\bar{p}$ annihilation at rest into $\pi^+\pi^-\pi^0$," Phys. Lett. B **469**, 270 (1999).
- [65] A. Abele *et al.* [Crystal Barrel Collaboration], " $\bar{p}d$ annihilation at rest into $\pi^+\pi^-\pi^-p_{\rm spectator}$," Phys. Lett. B **450**, 275 (1999).
- [66] D. V. Bugg, "Four sorts of meson," Phys. Rept. 397, 257 (2004).
- [67] P. Minkowski and W. Ochs, "B decays into light scalar particles and glueball," Eur. Phys. J. C 39, 71-86 (2005).
- [68] A. V. Anisovich, V. A. Nikonov, A. V. Sarantsev, V. V. Anisovich, M. A. Matveev, T. O. Vulfs, K. V. Nikonov and J. Nyiri, "Analysis of the meson-meson data in the framework of the dispersion D-matrix method," Phys. Rev. D 84, 076001 (2011).
- [69] V. A. Nikonov et al., "Note on branching ratios of overlapping resonances", unpublished (2018).
- [70] J. A. Oller, "The Mixing angle of the lightest scalar nonet," Nucl. Phys. A 727, 353-369 (2003).
- [71] E. Klempt, B. C. Metsch, C. R. Münz and H. R. Petry, "Scalar mesons in a relativistic quark model with instanton induced forces," Phys. Lett. B 361, 160-166 (1995).
- [72] A. Billoire, R. Lacaze, A. Morel and H. Navelet, "The Use of QCD in OZI Violating Radiative Decays of Vector Mesons," Phys. Lett. B 80, 381 (1979).
- [73] J. G. Körner, J. H. Kuhn, M. Krammer and H. Schneider, "Zweig Forbidden Radiative Orthoquarkonium Decays in Perturbative QCD," Nucl. Phys. B 229, 115 (1983).